SUPPLEMENTARY MATERIALS FOR

QUANTIFYING THE ROLE OF CLIMATE CHANGE IN DRIVING MASS CORAL BLEACHING

By Andrew J. Pershing, John F. Bruno, Joseph Giguere, and Alexandra Khrizman

https://doi.org/10.5670/oceanog.2026.e210

MATERIALS AND METHODS

DATA

This study uses sea surface temperatures from NOAA's Optimally Interpolated Sea Surface Temperature (OISST) dataset (Reynolds et al., 2007). The dataset has a 0.25° spatial resolution and is available daily, with 1982 the first full year. It blends a variety of satellite and in situ measurements to produce a gap-free product.

We use HadCRUT5 (Morice et al., 2021) as our indicator of global mean temperature (GMT). All global temperature values are reported relative to the 1850–1900 baseline used by the Intergovernmental Panel on Climate Change (IPCC). We represent the global climate of year Y by GMT15, ideally defined as the 15-year global mean temperature centered on Y. However, for Y >2017, we do not have sufficient observations to calculate GMT15 directly. Therefore, we compute the linear trend for GMT for the 30 prior years and then use the trend to project for year Y. The result is a close approximation (R2 = 0.99) to the 15-year average.

Below, we describe an analysis of the GMT15 values that cause bleaching risk to emerge above natural variability. For Figure 3, we identify the years when emergence has occurred or is likely to occur. This requires finding when global mean temperatures are expected to reach particular values. We use the average of the global mean temperatures in the IPCC AR6 report under SSP3.0-7 (IPCC, 2021). The year when 2.0° is reached only changes by a few years when comparing SSP3.0-7 to most other scenarios. The only exceptions are the scenarios with aggressive emission reductions that are unrealistic based on current global policies.

We use the Oceanic Niño Index (ONI) as our indicator of El Niño-Southern Oscillation (ENSO) state (Glantz and Ramirez, 2020; NOAA, 2025).

CORAL REEF ECOREGIONS

Our analysis is done on 100 ecoregions from the Marine Ecoregions of the World (MEOW; Spalding et al., 2007) database that contain coral reef ecosystems. We defined an ecoregion as one containing coral if that region contains one or more centroids of coral reefs identified by the UNEP World Conservation Monitoring Centre and associates (UNEP WCMC, 2025).

FOURTH GLOBAL MASS CORAL BLEACHING EVENT

Spady et al. (2026) identified countries and regions where bleaching was reported during the 2018–2025 period. They also identified the year when the peak heat stress in this region occurred. We manually mapped the reported bleaching locations to MEOW regions (Table S1). Small countries or islands are generally contained within a larger ecoregion, making the assignment clear. Larger locations such as "United States (Atlantic)" were assigned to multiple ecoregions.

OCEAN TEMPERATURE ATTRIBUTION

Attributing coral bleaching risk to climate change requires estimating conditions in a counterfactual world in which human caused climate change did not occur. We use the multi-method attribution approach developed by Gilford et al. (2022) and adapted by Giguere et al. (2024) for OISST. This approach works by modeling how changes in global mean temperature alter the frequency distribution of daily temperatures.

The Giguere approach begins by characterizing the distribution of daily temperatures during a recent reference period. We divide the year into 24 overlapping periods of 31 days centered on the first and the 15th of each month. For each OISST grid cell, we collect all observations from the 31 days from 1991 to 2020 and then summarize the frequency distribution by fitting a skew-normal distribution. This reference distribution is described by three parameters: L_{ref} (the location, analogous to the mean), S_{ref} (the scale, analogous to the variance), and A_{ref} (the skewness).

The reference distributions represent the climate circa 2008, which has *GMT15* = 0.88°C. We refer to this value as *GMTref*. The Giguere approach uses two empirical methods that rely on the observed relationship between local temperature and GMT as well as 13 global climate models to estimate the frequency distribution in other climates, especially the preindustrial climate (*GMT15* = 0.0°C).

For the empirical approaches, we use linear regression to model the relationship between the local temperatures during each seasonal period and GMT. We calculate the temperatures in the period corresponding to 21 evenly spaced quantiles (q) between 0.01 and 0.99 for the years 1982–2022. We then regress each of these time series against GMT to calculate β_q, the expected change in the qth quantile temperature due to a 1° change in GMT.

The values of β_q allow us to shift from the reference climate to any new climate specified by a global mean temperature. As in Giguere et al. (2024), we use two approaches. The first approach, referred to as the median method, assumes that the shape of the distribution does not change. Under this assumption,

$$SN_{median}(T, GMT15) = SN(T)[L_{ref} + \beta_{0.5}(GMT15\text{-}GMTref), S_{ref}, A_{ref}], \quad \text{(S1)}$$

where $SN(T)[L,S,A]$ is a skew-normal distribution.

We refer to the second approach as the quantile method, and it allows the shape of the distribution to change. To calculate the new skew normal distribution, we take the daily dataset used to develop the reference distribution and divide the data into the 21 quantiles. We shift each bin by $\beta_q(GMT15\text{-}GMTref)$, where β_q corresponds to the qth bin. We then refit the skew normal distribution, producing $SN_{quantile}(T, GMT15)$.

We also estimate the distribution of temperatures in a particular climate using 13 CMIP6 models (Table 1 in Giguere et al., 2024). For each model, we created a forced run by concatenating the historical (observed forcing) run with either SSP3-7.0 (preferred) or SSP5-8.5. The model output was interpolated to a standard 1° × 1° grid. Then, we applied a debiasing procedure (Lange, 2019) based on the observed data from the reference period. We applied the same debiasing to each model's pre-industrial control run. The debiasing brings each model more in line with the range of observed temperatures. However, our counterfactual temperature estimates, described below, are about relative changes in temperature between climates created by the same model. These two climates share the same bias, so any biases remaining after the debiasing step should have minimal impact.

For each pair of debiased model data, we calculate $SN_{forced}(T, GMT15)$ and $SN_{control}(T, Y)$. To find these distributions, we first find the year Y when the model's global mean temperature first exceeds *GMT15*. We then take the 31 years surrounding this year and fit the skew normal distribution to the same 24 periods of 31 days as above.

We then apply the Giguere et al. (2024) algorithm to estimate the counterfactual temperature ($T_{counter}$). For a temperature T observed in a climate with GMT15, we use the continuous distribution functions corresponding to $SN_{median}(T, GMT15)$, $SN_{quantile}(T, GMT15)$, and the 13 $SN_{forced}(T, GMT15)$ to find the probability of observing a temperature less than or equal to T. We then use SN_{median}(T, 0.0°), $SN_{quantile}$(T, 0.0°), and the 13 $SN_{control}$(T, 0.0°) estimates to find the temperature $T_{counter}$ that occurs with the same frequency. We get a single best estimate for $T_{counter}$ by averaging the model-based estimates, averaging the two empirical estimates, and then taking the average of these two averages.

CALCULATING CORAL BLEACHING RISK

NOAA's Coral Reef Watch (CRW) program developed a model of coral bleaching risk (Liu et al., 2014; Skirving et al., 2019) that assumes coral have adapted to historical temperatures in their location and that temperatures higher than typical are stressful. The model captures this logic by considering exposure to temperatures above the maximum climatological monthly temperature (*MxMT*).

We calculated *MxMT* for OISST following the CRW approach. Beginning with a time series of monthly means, we calculated the climatological mean for each month over the period 1985–2012. This climatology is centered on the year 1998.5. We also computed the trend τ_m (° yr^{-1}) for each month m over this period using linear regression. We then added τ_m(1998.5–1988.286) to each pixel in the climatology. This transforms the mean time period of the climatology to 1988.286. This is the mean of the years 1985–1990 plus 1993, the original climatology used by CRW. *MxMT* is then the maximum climatological monthly temperature at each pixel.

Stress to coral is presumed to be proportional to the accumulated exposure to temperatures above *MxMT*. The risk model represents stress as the degree heating weeks (DHW) summed over 12 weeks (84 days):

$$\text{DHW}(t) = \sum_{d=t-84}^{t} max(T(d) - (MxMT + 1), 0)/7. \quad \text{(S2)}$$

Based on empirical observations from previous bleaching events, CRW-established bleaching risk levels are then defined based on DHW (Heron et al., 2016; Manzello et al., 2025): moderate (DHW ≥ 4°-week) implies a risk of reef-wide bleaching, severe (DHW ≥ 8°-week) translates to a risk of mortality of sensitive species, and extreme (DHW ≥ 12°-week) risk of multi-species mortality. To highlight patterns at lower DWH, we split NOAA's "low" category into two bins: very low (DHW<1°-week) and low (1°-week ≤ DHW < 4°-week), corresponding to a risk of possible bleaching. For Figure 1, we split the extreme category into additional levels at steps of 4°-week.

We calculate DHW using both the observed temperatures in OISST and the counterfactual temperatures. We then compute $DHW_{max}(Y)$ = the maximum DHW for each year Y. These are averaged over the MEOW reef regions.

Using the standard reference period to define *MxMT* assumes that coral communities have not acclimatized or adapted to recent warming. To test this, we computed $DHW_{max}(2024)$ using *MxMT* defined by the 30 previous years: 1995–2022.

MODELING THE DRIVERS OF BLEACHING RISK

Previous studies have emphasized the importance of El Niño as a driver of large-scale bleaching events. To compare the influence of El Niño to changes in global mean temperatures, we fit a linear model to the DHW_{max} time series for each coral region:

$$DHW_{max}(Y) = a{*}GMT15(Y) + b{*}ONI(Y\text{-}L) + c, \qquad \text{(S3)}$$

where L is a lag in months. For each region, we tested L from 0 to 12 months and selected the value that gives the best relationship.

For locations where both terms were significant, we compared the strength of the two drivers by considering a strong El Niño (ONI = 2) and then finding the *GMT15* necessary to meet or exceed the influence of ONI (GMT_{equiv}) on DHW_{max}:

$$GMT_{equiv}(\text{ONI}) = \text{ONI}{*}b/a.$$

For all locations, with a significant *GMT15* term, we solved for the *GMT15* value that produces a DHW_{max} equivalent to twice the standard deviation of the regression model (ONI assumed equal to zero).

SUPPLEMENTARY TEXT

Figure S1 shows the spatial distribution of the linear modeling results. Regions in red have only a significant ($p < 0.05$) *GMT15* term. Regions in yellow have only a significant ONI term, and regions in orange have both. The parameters for each region are available in Table S1.

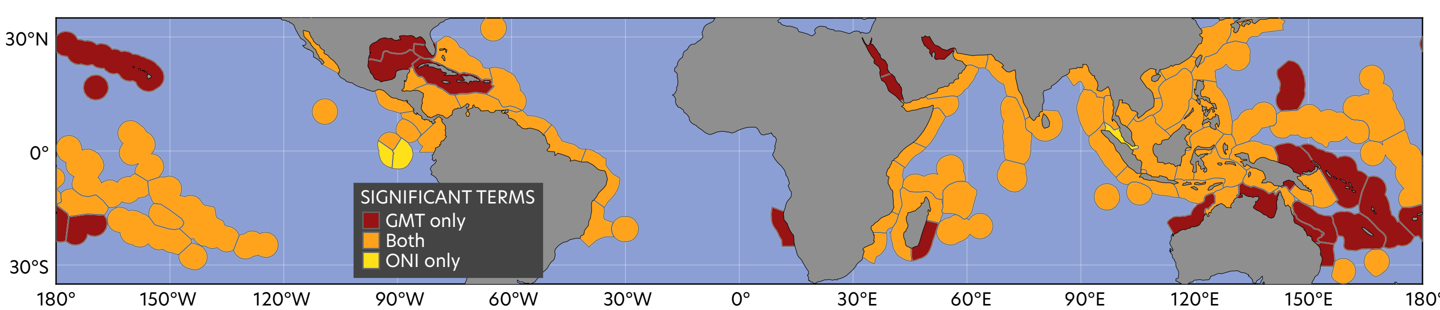

FIGURE S1. Map showing the significant terms from the statistical modeling. For each region, we modeled DHW_{max} as a linear function of both Oceanic Niño Index (ONI) and global mean temperature (GMT). In the red regions, only the GMT term was significant. In the yellow regions, only the ONI term was significant. Both terms were significant in the orange regions. Specific parameter values are in Table S1.

TABLE S1. Results of the statistical modeling of DHW_{max} as a function of ONI and GMT15. M = month when maximum temperatures occur. Observed and Counterfactual DHWmax refer to the values observed during the most recent event (see Figure 1). R2 = coefficient of determination. SD = model residual standard deviation. p GMT and p ONI = significance of the terms. a, b, and c = model parameters for (S3). lag = the number of months shift in ONI that produces the best model. GMT_{equiv} = the GMT15 value required to match ONI = 2. Y_{equiv} = the year when GMT_{equiv} occurs. GMT_{emerge} = the GMT15 value required to match 2SD. Y_{emerge} = the year when GMT_{emerge} occurs.

MEOW Code	Ecoregion	M	Observed DHW_{max}	Counterfactual DHW_{max}	R2	SD	p GMT	p ONI	a = GMT	b = ONI	c	lag	GMT_{equiv}	Y_{equiv}	GMT_{emerge}	Y_{emerge}
20118	Malacca Strait	6	4.9	0.5	0.40	0.97	0.32	0.00	0.56	0.67	0.71	5	2.41	2060	3.49	2089
20174	Western Galapágos Islands	3	9.2	2.1	0.31	4.78	0.25	0.00	3.23	3.19	1.42	1	1.98	2047	2.96	2075
20173	Eastern Galapágos Islands	3	11.4	2.3	0.36	4.69	0.06	0.00	5.19	3.47	0.38	1	1.34	2025	1.81	2041
20140	Arnhem Coast to Gulf of Carpenteria	6	7.2	0.6	0.18	1.46	0.05	0.07	1.66	−0.64	1.25	0	0.77	2000	1.76	2040
20139	Arafura Sea	7	7.0	0.5	0.23	1.66	0.03	0.03	2.04	−0.80	1.75	0	0.79	2002	1.63	2036
20090	Arabian (Persian) Gulf	8	10.9	0.1	0.20	2.90	0.03	0.08	3.61	−1.14	−0.43	1	0.63	1992	1.61	2035
25190	Namib	2	17.7	5.6	0.12	5.04	0.03	0.18	6.43	1.38	0.63	11	0.43	1946	1.57	2033
20155	Line Islands	6	13.6	1.5	0.45	3.97	0.03	0.00	5.25	3.56	0.15	4	1.36	2026	1.51	2031
20169	Cocos Islands	3	6.5	0.4	0.50	2.20	0.02	0.00	3.08	2.17	−0.38	1	1.41	2028	1.43	2028
20077	Trindade and Martin Vaz Islands	3	11.3	2.4	0.26	2.39	0.01	0.00	3.40	0.95	−1.72	3	0.56	1991	1.40	2028
20168	Nicoya	4	8.2	1.2	0.46	2.23	0.01	0.00	3.26	2.04	−0.30	2	1.25	2022	1.37	2026
20126	Palawan/North Borneo	5	5.8	0.1	0.31	1.18	0.01	0.00	1.90	0.60	−0.22	7	0.64	1993	1.24	2022
20172	Northern Galapágos Islands	3	10.1	0.8	0.56	3.14	0.01	0.00	5.08	3.51	−0.49	1	1.38	2027	1.24	2021
20095	East African Coral Coast	3	9.4	0.2	0.47	1.54	0.01	0.00	2.47	1.54	−0.47	6	1.24	2021	1.24	2021
20143	Central and Southern Great Barrier Reef	2	8.9	0.9	0.19	2.28	0.00	0.22	3.85	0.57	−0.86	11	0.30	1941	1.18	2020
20076	Eastern Brazil	3	8.4	0.9	0.30	1.65	0.00	0.00	2.84	0.68	−1.28	3	0.48	1988	1.16	2019
20133	Northeast Sulawesi	6	4.6	0.0	0.32	0.93	0.00	0.00	1.62	0.59	−0.01	9	0.73	1999	1.14	2018
20117	Sunda Shelf/Java Sea	6	5.2	0.1	0.41	0.89	0.00	0.00	1.57	0.59	0.06	5	0.75	1999	1.13	2018
20131	Banda Sea	10	4.1	0.0	0.32	0.86	0.00	0.03	1.56	−0.42	0.85	3	0.54	1990	1.11	2017
20075	Northeastern Brazil	4	17.6	0.6	0.28	2.80	0.00	0.01	5.09	0.99	−2.58	5	0.39	1945	1.10	2017
20130	Papua	8	6.7	0.2	0.41	1.31	0.00	0.00	2.45	−0.75	0.22	0	0.61	1992	1.07	2016
20088	Southern Red Sea	9	15.4	0.7	0.22	2.51	0.00	0.17	4.83	0.59	−2.13	0	0.24	1938	1.04	2015
20170	Panama Bight	5	19.3	3.3	0.41	4.87	0.00	0.00	9.56	3.74	−1.84	3	0.78	2001	1.02	2014
20156	Phoenix/Tokelau/Northern Cook Islands	7	18.5	4.3	0.46	2.96	0.00	0.00	5.78	1.94	−1.32	8	0.67	1996	1.03	2014
20119	Southern Java	3	7.3	0.3	0.49	2.25	0.00	0.00	4.46	1.77	−1.03	2	0.79	2002	1.01	2012
20120	Cocos-Keeling/Christmas Island	4	10.9	0.4	0.42	2.55	0.00	0.00	5.10	1.70	−1.28	6	0.67	1996	1.00	2012
20167	Chiapas-Nicaragua	6	8.6	0.5	0.40	1.63	0.00	0.00	3.42	1.56	−0.77	3	0.91	2008	0.96	2011
20202	Tweed-Moreton	2	16.7	3.3	0.25	3.27	0.00	0.08	6.69	0.91	−2.38	0	0.27	1939	0.98	2011
20111	Western Sumatra	5	8.4	0.2	0.50	1.61	0.00	0.00	3.43	1.28	−0.52	4	0.74	1999	0.94	2010
20158	Tuamotus	3	5.9	0.1	0.36	1.38	0.00	0.00	3.03	0.89	−1.18	6	0.58	1991	0.91	2008
20115	Gulf of Thailand	5	9.1	0.3	0.49	1.47	0.00	0.00	3.23	1.11	−1.15	4	0.68	1997	0.91	2007
20159	Rapa-Pitcairn	2	9.5	2.6	0.50	2.01	0.00	0.00	4.49	−1.01	−0.90	2	0.45	1987	0.89	2006
20153	Marshall Islands	9	4.5	0.0	0.28	1.23	0.00	0.04	2.79	0.62	−0.99	5	0.45	1986	0.88	2006
20101	Bight of Sofala/Swamp Coast	3	6.2	0.1	0.33	1.71	0.00	0.00	3.87	0.85	−0.94	1	0.44	1985	0.88	2006
20151	Lord Howe and Norfolk Islands	2	12.8	1.8	0.31	2.23	0.00	0.01	5.00	0.80	−1.94	1	0.32	1941	0.89	2006
20149	New Caledonia	2	9.6	0.8	0.29	2.13	0.00	0.56	4.88	0.19	−1.37	12	0.08	1882	0.87	2005
20105	Maldives	4	6.7	0.0	0.47	1.38	0.00	0.00	3.19	1.25	−1.20	7	0.79	2001	0.86	2004

MEOW Code	Ecoregion	M	Observed DHW_{max}	Counterfactual DHW_{max}	R2	SD	p GMT	p ONI	a = GMT	b = ONI	c	lag	GMT_{equiv}	Y_{equiv}	GMT_{emerge}	Y_{emerge}
20128	Sulawesi Sea/Makassar Strait	6	4.5	0.1	0.32	0.92	0.00	0.02	2.20	0.38	0.03	9	0.35	1943	0.84	2004
20091	Gulf of Oman	6	8.4	0.8	0.33	1.51	0.00	0.01	3.62	0.86	−1.02	3	0.47	1988	0.83	2003
20141	Bonaparte Coast	9	6.3	0.2	0.33	1.54	0.00	0.01	3.72	0.69	0.02	12	0.37	1945	0.83	2003
25154	Gilbert/Ellis Islands	9	11.7	0.4	0.38	2.45	0.00	0.00	5.94	1.18	−1.61	11	0.40	1945	0.83	2003
20102	Delagoa	2	10.6	0.6	0.33	1.66	0.00	0.04	4.07	0.68	−1.48	11	0.34	1942	0.81	2003
25152	Hawaii	9	9.0	0.1	0.31	1.79	0.00	0.11	4.39	0.70	−2.23	4	0.32	1941	0.81	2003
20099	Southeast Madagascar	2	13.3	0.3	0.32	2.50	0.00	0.08	6.04	0.89	−2.13	11	0.29	1941	0.83	2003
20106	Chagos	4	7.1	0.0	0.45	1.70	0.00	0.00	4.28	1.39	−1.81	7	0.65	1994	0.79	2002
20104	South India and Sri Lanka	4	8.1	0.5	0.52	1.42	0.00	0.00	3.54	1.11	−1.51	3	0.63	1992	0.80	2002
20161	Society Islands	3	6.4	0.0	0.37	1.47	0.00	0.00	3.68	0.80	−1.42	1	0.44	1946	0.80	2002
20138	Gulf of Papua	2	13.0	1.0	0.33	2.49	0.00	0.11	6.31	0.69	−1.06	5	0.22	1937	0.79	2002
25147	Fiji Islands	2	9.9	0.0	0.40	2.04	0.00	0.11	5.15	−0.52	−1.32	12	0.20	1936	0.79	2002
20129	Halmahera	7	5.7	0.0	0.50	1.27	0.00	0.00	3.25	−0.98	−0.74	0	0.60	1992	0.78	2001
20132	Lesser Sunda	5	8.2	1.1	0.44	1.66	0.00	0.00	4.33	1.23	−0.34	8	0.57	1991	0.76	2000
20121	South Kuroshio	7	16.7	3.8	0.39	2.73	0.00	0.00	7.13	1.61	−2.99	10	0.45	1988	0.77	2000
20134	Bismarck Sea	7	10.4	0.2	0.44	1.76	0.00	0.07	4.61	−0.79	−0.91	2	0.34	1943	0.77	2000
20051	Central Kuroshio Current	8	17.4	5.4	0.36	3.00	0.00	0.01	7.79	1.29	−3.51	11	0.33	1942	0.77	2000
20146	Tonga Islands	2	8.7	0.3	0.43	2.00	0.00	0.10	5.22	−0.52	−1.08	0	0.20	1936	0.77	2000
20087	Northern and Central Red Sea	8	15.0	0.3	0.35	2.73	0.00	0.09	7.03	0.68	−3.25	10	0.19	1933	0.78	2000
20165	Clipperton	5	6.9	0.0	0.39	1.32	0.00	0.00	3.64	1.02	−1.32	1	0.56	1991	0.72	1999
20109	Andaman and Nicobar Islands	5	10.8	2.7	0.47	1.93	0.00	0.00	5.22	1.25	−2.17	4	0.48	1988	0.74	1999
20160	Southern Cook/Austral Islands	3	11.6	1.3	0.45	2.39	0.00	0.04	6.55	−1.08	−2.28	8	0.33	1942	0.73	1999
20123	Mariana Islands	8	14.0	0.2	0.44	2.80	0.00	0.10	7.42	−0.91	−2.81	0	0.24	1938	0.75	1999
20150	Coral Sea	2	12.9	1.1	0.37	2.93	0.00	0.14	8.14	0.89	−2.83	11	0.22	1937	0.72	1999
20100	Western and Northern Madagascar	3	7.2	0.2	0.46	1.46	0.00	0.00	4.12	1.11	−0.98	6	0.54	1990	0.71	1998
20110	Andaman Sea Coral Coast	5	11.7	1.3	0.48	2.00	0.00	0.00	5.64	1.28	−2.27	4	0.45	1988	0.71	1998
20094	Northern Monsoon Current Coast	4	14.3	1.4	0.49	2.19	0.00	0.00	6.14	1.46	−3.10	3	0.47	1988	0.71	1998
20148	Vanuatu	3	6.2	0.1	0.43	1.22	0.00	0.37	3.48	−0.26	−0.56	11	0.15	1932	0.70	1998
20144	Exmouth to Broome	4	11.8	1.5	0.39	1.81	0.00	0.09	5.30	0.60	−1.57	8	0.22	1938	0.68	1997
20116	Southern Vietnam	5	11.2	0.5	0.53	1.83	0.00	0.00	5.40	1.33	−2.24	4	0.49	1989	0.68	1996
20127	Eastern Philippines	6	9.2	0.2	0.44	1.77	0.00	0.00	5.36	1.02	−2.16	9	0.38	1945	0.66	1996
20068	Western Caribbean	9	13.5	0.1	0.39	2.47	0.00	0.04	7.28	1.09	−4.07	6	0.30	1941	0.68	1996
20072	Amazonia	6	16.2	0.1	0.42	2.50	0.00	0.01	7.50	0.89	−3.81	5	0.24	1938	0.67	1996
20124	East Caroline Islands	9	11.9	0.0	0.42	2.06	0.00	0.04	6.30	0.73	−2.58	12	0.23	1938	0.65	1994
20136	Solomon Sea	2	15.1	2.5	0.51	2.19	0.00	0.02	6.78	−0.64	−1.77	2	0.19	1933	0.65	1994
20070	Floridian	8	15.6	1.6	0.42	2.37	0.00	0.23	7.40	0.58	−4.08	5	0.16	1932	0.64	1994
20063	Bahamian	9	11.5	0.1	0.43	1.81	0.00	0.01	5.72	0.98	−3.23	6	0.34	1943	0.63	1993
20065	Greater Antilles	9	17.2	0.1	0.42	2.78	0.00	0.06	8.73	1.07	−4.86	6	0.25	1938	0.64	1993
20125	West Caroline Islands	7	12.7	0.1	0.58	2.07	0.00	0.00	6.69	−1.65	−2.32	0	0.49	1989	0.62	1992
20114	South China Sea Oceanic Islands	5	10.9	0.5	0.52	1.89	0.00	0.00	6.00	1.23	−2.38	7	0.41	1946	0.63	1992
20142	Torres Strait Northern Great Barrier Reef	2	12.9	1.1	0.46	2.38	0.00	0.01	7.73	1.22	−2.48	11	0.32	1941	0.62	1992

MEOW Code	Ecoregion	M	Observed DHW_{max}	Counterfactual DHW_{max}	R2	SD	p GMT	p ONI	a = GMT	b = ONI	c	lag	GMT_{equiv}	Y_{equiv}	GMT_{emerge}	Y_{emerge}
20052	East China Sea	8	17.8	5.1	0.44	2.77	0.00	0.03	8.93	1.06	−4.38	11	0.24	1938	0.62	1992
20069	Southern Gulf of Mexico	8	15.1	0.6	0.43	2.56	0.00	0.08	8.14	0.92	−4.31	5	0.23	1938	0.63	1992
20043	Northern Gulf of Mexico	8	15.8	1.6	0.44	2.61	0.00	0.06	8.38	0.79	−4.03	6	0.19	1933	0.62	1992
20096	Seychelles	4	12.9	0.2	0.60	1.81	0.00	0.00	6.39	1.51	−3.04	3	0.47	1988	0.57	1991
20060	Cortezian	8	9.9	0.2	0.49	2.72	0.00	0.00	9.64	1.69	−3.30	0	0.35	1943	0.56	1991
20098	Mascarene Islands	2	19.1	0.6	0.50	2.99	0.00	0.00	10.61	1.66	−5.09	5	0.31	1941	0.56	1991
20137	Southeast Papua New Guinea	1	17.7	2.4	0.50	2.64	0.00	0.03	9.37	0.80	−3.42	12	0.17	1933	0.56	1991
20089	Gulf of Aden	6	5.6	0.3	0.55	1.02	0.00	0.00	3.73	0.80	−1.46	9	0.43	1946	0.54	1990
20157	Samoa Islands	3	18.9	1.1	0.52	3.00	0.00	0.00	11.10	2.29	−5.15	0	0.41	1946	0.54	1990
20093	Central Somali Coast	4	8.4	0.4	0.54	1.43	0.00	0.00	5.21	1.01	−2.37	7	0.39	1945	0.55	1990
20108	Northern Bay of Bengal	7	8.3	0.7	0.52	1.63	0.00	0.01	6.18	0.59	−2.43	6	0.19	1933	0.53	1990
20135	Solomon Archipelago	6	9.8	0.4	0.51	1.56	0.00	0.17	5.79	0.37	−1.65	9	0.13	1931	0.54	1990
20064	Eastern Caribbean	9	23.0	0.1	0.55	3.64	0.00	0.01	14.78	2.07	−8.05	6	0.28	1940	0.49	1989
20062	Bermuda	8	17.4	0.0	0.55	2.87	0.00	0.01	11.71	1.51	−6.61	5	0.26	1939	0.49	1989
20097	Cargados Carajos/Tromelin Island	3	16.3	0.3	0.63	2.58	0.00	0.00	10.66	2.53	−5.30	6	0.47	1988	0.48	1988
20112	Gulf of Tonkin	7	13.9	1.5	0.57	2.77	0.00	0.01	11.51	1.18	−5.16	5	0.20	1937	0.48	1988
20067	Southwestern Caribbean	9	20.9	0.5	0.59	3.10	0.00	0.03	13.62	1.43	−7.10	6	0.21	1937	0.46	1988
20113	Southern China	8	15.3	2.4	0.57	2.49	0.00	0.01	10.29	0.95	−4.62	7	0.18	1933	0.48	1988
20071	Guianan	9	17.1	0.2	0.57	2.69	0.00	0.04	11.19	0.76	−5.52	8	0.14	1932	0.48	1988
20066	Southern Caribbean	9	23.4	0.9	0.57	3.74	0.00	0.03	15.43	1.03	−7.61	9	0.13	1932	0.48	1988
20103	Western India	6	10.7	0.8	0.64	1.66	0.00	0.00	7.80	0.92	−3.99	5	0.24	1938	0.43	1946
20092	Western Arabian Sea	5	7.0	0.1	0.66	1.24	0.00	0.00	6.07	0.91	−2.93	3	0.30	1941	0.41	1945